



# Selenoprotein W controls epidermal growth factor receptor surface expression, activation and degradation via receptor ubiquitination



Zeynep Alkan<sup>a,\*</sup>, Frank L. Duong<sup>b</sup>, Wayne C. Hawkes<sup>a</sup>

<sup>a</sup> USDA-ARS Western Human Nutrition Research Center, 430 West Health Sciences Drive, University of California, Davis, CA 95616, USA

<sup>b</sup> Cedars Sinai Medical Center, Department of Medicine, 8750 Beverly Boulevard, Atrium 103, West Hollywood, CA 90048, USA

## ARTICLE INFO

### Article history:

Received 14 November 2014

Received in revised form 2 February 2015

Accepted 16 February 2015

Available online 23 February 2015

### Keywords:

Selenium

Selenoprotein W

Epidermal growth factor receptor

Ubiquitination

Cancer

## ABSTRACT

Epidermal growth factor (EGF) receptor (EGFR) is the founding member of the ErbB family of growth factor receptors that modulate a complex network of intracellular signaling pathways controlling growth, proliferation, differentiation, and motility. Selenoprotein W (SEPW1) is a highly conserved, diet-regulated 9 kDa thioredoxin-like protein required for normal cell cycle progression. We report here that SEPW1 is required for EGF-induced EGFR activation and that it functions by suppressing EGFR ubiquitination and receptor degradation. SEPW1 depletion inhibited EGF-dependent cell cycle entry in breast and prostate epithelial cells. In prostate cells, SEPW1 depletion decreased EGFR auto-phosphorylation, while SEPW1 overexpression increased EGFR auto-phosphorylation. SEPW1 depletion increased the rate of EGFR degradation, which decreased total and surface EGFR and suppressed EGF-dependent EGFR endocytosis, EGFR dimer formation, and activation of EGF-dependent pathways. EGFR ubiquitination was increased in SEPW1-depleted cells – in agreement with the increased rate of EGFR degradation, and suggests that SEPW1 suppresses EGFR ubiquitination. Ubiquitination-directed lysosomal degradation controls post-translational EGFR expression and is dysregulated in many cancers. Thus, suppression of EGFR ubiquitination by SEPW1 may be related to the putative increase in cancer risk associated with high selenium intakes. Knowledge of the mechanisms underlying SEPW1's regulation of EGFR ubiquitination may reveal new opportunities for nutritional cancer prevention or cancer drug development.

Published by Elsevier B.V.

## 1. Introduction

Epidermal growth factor (EGF) is a 53 amino acid polypeptide growth factor that regulates cell growth, proliferation and differentiation [1,2]. The EGF receptor (EGFR) is a receptor tyrosine kinase of the ErbB family, so-named because they are homologous with the erythroblastic leukemia viral oncogene. Four members of the oncogenic ErbB family have been identified: EGFR (ErbB1, HER1), ErbB2 (HER2), ErbB3 (HER3), and ErbB4 (HER4). EGFR was the first growth factor receptor to be identified in cancer cells and is considered a human proto-oncogene. EGFR is expressed in approximately one-third of cancers and the EGFR system is constitutively activated in many tumors. EGFR is activated by binding of various peptide growth factors, including EGF, transforming growth factor alpha (TGF $\alpha$ ), amphiregulin, and heparin-binding EGF-like growth factor. EGFR ligands are produced by proteolytic cleavage from the extracellular domains of cell surface proteins or secreted precursor proteins. Most of the EGF family of growth

factors are biologically active only in their soluble secreted forms, but some are also active as transmembrane precursor molecules [3]. Thus, EGFR is involved in endocrine, paracrine, and autocrine signaling mechanisms responding to systemic, local tissue, and intercellular cues. The EGFR network regulates growth, proliferation, differentiation and motility through pathways such as extracellular signal-regulated kinase (ERK), phosphatidylinositol-3-kinase (PI3K), mitogen-activated protein kinase (MAPK), and signal transducer and activator of transcription [4]. The EGFR network crosstalks extensively with other receptor tyrosine kinases, G-protein coupled receptors, and cytokine receptors, and is a major hub in the extracellular signaling network [5–8].

Ligand binding leads to asymmetric EGFR dimerization, induction of the tyrosine kinase activity, auto-phosphorylation of the receptor, binding of cytoplasmic cofactors, internalization of the EGF-receptor complex, and initiation of a complex network of signaling cascades. Phosphorylated EGFR binds the E3 ubiquitin ligase Cbl, which adds ubiquitin at several lysine residues [9]. The ubiquitinated receptor is recognized by ubiquitin-binding domains in several members of the endosomal sorting complex for retrograde transport (“ESCRT”) protein complex. Ubiquitinated EGFR is endocytosed and trafficked to lysosomes for degradation, or alternatively, EGFR can be de-ubiquitinated and recycled to the plasma membrane for re-use [10].

Abbreviations: ANOVA, analysis of variance; CHX, cycloheximide; BS<sup>3</sup>, bis(sulfosuccinimidyl)suberate; SE, standard error of the mean; Sec, selenocysteine

\* Corresponding author. Tel.: +1 530 752 4725.

E-mail address: [zeynep.alkan@ars.usda.gov](mailto:zeynep.alkan@ars.usda.gov) (Z. Alkan).

The ubiquitination state of the receptor determines the relative rates of EGFR degradation and recycling, and ultimately, the amount of EGFR expressed on the cell's surface.

Selenoprotein W (SEPW1) is a 9 kDa thioredoxin-like protein with a selenocysteine (Sec) residue at the active site. SEPW1 is ubiquitously expressed and conserved in all major phyla except higher plants and fungi. SEPW1 is cell cycle regulated, is required for cell cycle progression, and is the only selenoprotein whose mRNA was increased by sub-micromolar concentrations of selenium in cultured human cells [11]. We found that G1-phase cell cycle arrest from SEPW1 depletion is mediated by phosphorylation of the p53 tumor suppressor protein via p38 MAPK and JNK2 under control of MKK4 [12–14]. We report here that SEPW1 is required for activation of EGFR upstream of MKK4 for the EGF-stimulated proliferation of prostate and breast epithelial cells. SEPW1 suppresses EGFR ubiquitination, which decreases lysosomal degradation and increases surface EGFR concentration and EGF responsiveness.

## 2. Materials and methods

### 2.1. Cell culture

RWPE-1 and MCF-10A cells were obtained from the American Type Culture Collection ("ATCC", Manassas, VA) and maintained in serum-free medium supplemented with EGF as described before [11].

### 2.2. siRNA transfections

Cells were transfected in medium containing either 0 or 5 ng/mL EGF per previously established protocols [14] with Silencer Select siRNAs targeting SEPW1 (s361, s363) or non-targeting control siRNAs #1 and #2 (ABI, Foster City, CA). Data identified as "SEPW1 siRNA" refers to siRNA s361, unless indicated otherwise.

### 2.3. SEPW1 overexpression vector transfections

Approximately 300,000 RWPE-1 cells per well were seeded in six well dishes on the day prior to transfection. The cells in each well were transiently transfected with either 2  $\mu$ g SEPW1 *TrueClone* cDNA clone in a p-CMV6-Neo vector or the empty vector (Origene, Rockville, MD) with 10  $\mu$ L Superfect Reagent (QIAGEN, Valencia, CA) per manufacturer's instructions. Three hours after the addition of transfection complexes, the cells were rinsed and supplied with fresh medium.

### 2.4. Cell cycle analysis

Propidium iodide staining of cellular DNA, flow cytometry, and data analysis were performed as described before [14].

### 2.5. Western blots

Western blot analyses were conducted using antibodies targeting the following proteins: EGFR (pan-specific), p-Tyr-992-EGFR, p-Tyr-1045-EGFR, p-Tyr-1068 EGFR, ubiquitin (Cell Signaling Technologies, Danvers, MA),  $\beta$ -actin,  $\beta$ -tubulin, and vinculin (Sigma). PVDF membranes were stripped with Restore Plus reagent (Pierce, Rockford, IL), and re-probed as needed. The immunoblots were imaged with a ChemiDoc XRS+ system (BioRad, Hercules, CA), and densitometry was performed with ImageLab software (BioRad). The chemiluminescence of each protein band was normalized to the average chemiluminescence of all the bands of the same protein from the corresponding immunoblot prior to combined statistical analysis from multiple blots.

### 2.6. Proteome profiler human phospho-MAPK arrays

Two hundred  $\mu$ g total protein from each lysate was hybridized to Proteome Profiler Human Phospho-MAPK antibody arrays (R&D Systems, Minneapolis, MN) per manufacturer's protocol, and all the arrays were imaged simultaneously with the ChemiDoc XRS+ System. Densitometry was conducted with ImageLab software, and all the densitometry values were divided by 1000 for data presentation simplification. The average intensity of two negative control spots on each array was subtracted from the protein kinase spot intensities of the corresponding array for background correction.

### 2.7. Chemical crosslinking of cell surface receptors

EGF-starved cells were treated with 100 ng/mL EGF for 30 min at 4 °C, placed on ice, washed three times with ice-cold PBS, and then incubated with the non-membrane permeable crosslinking reagent bis(sulfosuccinimidyl)suberate (BS<sup>3</sup>, Pierce), 3 mM, in PBS for 2 h at 4 °C. Excess BS<sup>3</sup> was quenched by addition of 1 M Tris-HCl, pH 7.4 to a final concentration of 20 mM and holding at 4 °C for 15 min. Cells were then washed with PBS, lysed, and the lysates analyzed by immunoblotting.

### 2.8. Fluorescent EGF internalization

Cells transfected and grown on coverslips were starved of EGF overnight and then stimulated with medium containing 970 ng/mL Alexa Fluor 488 streptavidin-biotin conjugated EGF (equivalent to 100 ng/mL EGF; Invitrogen), washed with PBS, fixed in ice-cold 100% methanol for 4 min, counter-stained with 4',6-diamidino-2-phenylindole (DAPI, Sigma), and mounted on slides using SlowFade reagent (Invitrogen). The images were acquired on an FV1000 laser scanning confocal microscope (Olympus, Center Valley, PA). Total background-corrected Alexa Fluor 488 intensity of each image was measured with ImageJ software [43,44] and fluorescent EGF signal per cell was calculated by dividing the whole image signal intensity by the total number of cells in the image.

### 2.9. Measurement of surface receptor expression

Cell pellets were washed with ice-cold PBS containing 2 mM EDTA and 1% FBS (blocking buffer), fixed in PBS with 4% paraformaldehyde for 20 min on ice, washed again, and counted. Approximately 200,000 cells per sample were incubated with 1:50 EGFR antibody Ab-3 (Thermo Scientific) diluted in equal volumes of cold blocking buffer, washed, and then stained with 1:200 Alexa Fluor 488 conjugated anti-mouse antibody (Cell Signaling Technology). At least 40,000 events per sample were collected on a FACSCanto flow cytometer (BD Biosciences), and FITC area peak mean intensities were calculated by FACSDiva software (BD Biosciences).

### 2.10. Receptor immunoprecipitation

Cells were lysed with M-Per buffer containing HALT protease and phosphatase inhibitor cocktails (Pierce), and 400  $\mu$ g total protein from each lysate were incubated with 1:100 EGFR antibody D38B1 (Cell Signaling Technology) in equal buffer volume for 1 h at 4 °C on a rocker. 50  $\mu$ L Protein A/G Agarose Plus beads (Santa Cruz Biotechnology) were added to each sample prior to overnight incubation at 4 °C with rocking. The beads were washed five times with PBS and then boiled in reducing sample loading buffer for 5 min, and the supernatants were analyzed by immunoblotting.

### 2.11. Microarray analysis

RWPE-1 cells were transfected with 0.2% siPORT Amine reagent (ABI) and 30 nM of one of three Silencer SEPW1 siRNAs (#42029, 41942, or 41846), or with 30 nM non-targeting control siRNA AM4635 (ABI). RNA was isolated and analyzed with whole genome DNA microarrays (Affymetrix HG-U133 Plus 2.0) as described previously [14]. There were 664 genes differentially expressed ( $p < 0.002$ ) in SEPW1-depleted cells.

### 2.12. Statistical analysis

Each experiment was performed at least twice, and two biological replicates per condition were analyzed in each experiment, except for immunoblots. In the case of Western blot analyses, every independent experiment contained one biological replicate. No technical replicates were run. Data from different treatments were compared using two-way analysis of variance (ANOVA) or *t*-tests with SigmaPlot 12.3 software (Systat). Estimates of experimental variability are expressed as standard error of the mean (SE). Between-group comparisons were analyzed with Tukey's test. A probability of  $\leq 0.05$  was considered significant.

## 3. Results

### 3.1. SEPW1 depletion blocks EGF-stimulated cell cycle entry

Because G1 arrest from SEPW1 depletion was first observed in cells that only proliferate in the presence of added EGF, we speculated that SEPW1 might be required for EGF-stimulated cell cycle entry. When grown continuously in 5 ng/mL EGF, 31.4% of RWPE-1 cells were in S-phase versus 5.1% without EGF, indicating 26.3% entered the cell cycle in response to EGF (Table 1). In contrast, only 8.2% of SEPW1-depleted RWPE-1 cells entered the cell cycle in response to EGF; less than one-third the rate in control cells. We observed a similar response in breast cells: When grown continuously in 5 ng/mL EGF, 14.6% of MCF-10A cells were in S-phase versus 6.7% without EGF, indicating 7.9% entered the cell cycle in response to EGF (Table 2). However, only 4.4% of SEPW1-depleted MCF-10A cells entered the cell cycle in response to EGF; about half the rate in control cells. Accordingly, we conclude that SEPW1 is required for EGF-stimulated cell cycle entry in both prostate and breast epithelial cells.

### 3.2. SEPW1 depletion decreases EGFR auto-phosphorylation and total EGFR

EGF binding stimulates auto-phosphorylation of several Tyr residues in the cytoplasmic domain of EGFR. Phosphorylation of Tyr-992, Tyr-

**Table 1**  
SEPW1 silencing decreases EGF-stimulated S-phase entry in RWPE-1 prostate epithelial cells.

siRNA treatment	[EGF], ng/mL	Percentage of cells ( $\pm$ SEM)		
		G0 and G1	S-phase	G2 and M
No transfection	0	83.1 $\pm$ 0.2	9.8 $\pm$ 0.2	7.1 $\pm$ 0.1
	5	60.6 $\pm$ 1.9	32.7 $\pm$ 1.2	6.6 $\pm$ 0.8
Non-targeting control siRNA	0	86.1 $\pm$ 0.9 <sup>a</sup>	5.1 $\pm$ 0.3 <sup>a</sup>	8.8 $\pm$ 1.2 <sup>a</sup>
	5	61.7 $\pm$ 0.3 <sup>b</sup>	31.4 $\pm$ 0.1 <sup>b</sup>	6.9 $\pm$ 0.2 <sup>a,c</sup>
SEPW1 siRNA	0	82.4 $\pm$ 3.3 <sup>a</sup>	11.1 $\pm$ 3.6 <sup>c</sup>	6.4 $\pm$ 0.3 <sup>b</sup>
	5	74.8 $\pm$ 1.6 <sup>c</sup>	19.3 $\pm$ 0.2 <sup>d</sup>	5.9 $\pm$ 1.4 <sup>b,c</sup>

Three days after transfection, cells were fixed, stained with propidium iodide, and their DNA contents measured by flow cytometry. Cell cycle phase distributions were calculated with ModFit LT 3.0 software. The experiment was conducted twice and two biological replicates were analyzed in each experiment. The data shown are the means  $\pm$  SE. SEPW1 siRNA-treated cells were compared to the control cells with a two-way ANOVA and Tukey's multiple comparisons test. Means within a column not sharing a superscript are significantly different ( $p < 0.05$ ). Representative pseudo-color density plots of events and cellular DNA content are shown in Supplemental Figure S1.

**Table 2**

SEPW1 silencing decreases EGF-stimulated S-phase entry in MCF-10A breast epithelial cells.

siRNA treatment	[EGF], ng/mL	Percentage of cells ( $\pm$ SEM)		
		G0 and G1	S-phase	G2 and M
No transfection	0	85.6 $\pm$ 0.0	9.4 $\pm$ 0.1	5.0 $\pm$ 0.1
	5	72.2 $\pm$ 0.9	18.2 $\pm$ 0.6	9.6 $\pm$ 0.2
Non-targeting control siRNA	0	89.1 $\pm$ 0.1 <sup>a</sup>	6.7 $\pm$ 0.3 <sup>a</sup>	4.2 $\pm$ 0.2 <sup>a</sup>
	5	77.5 $\pm$ 0.0 <sup>b</sup>	14.6 $\pm$ 0.1 <sup>b</sup>	7.8 $\pm$ 0.1 <sup>b</sup>
SEPW1 siRNA	0	91.5 $\pm$ 0.2 <sup>c</sup>	5.0 $\pm$ 0.0 <sup>c</sup>	3.5 $\pm$ 0.1 <sup>a</sup>
	5	83.6 $\pm$ 0.5 <sup>d</sup>	9.4 $\pm$ 0.2 <sup>d</sup>	6.9 $\pm$ 0.3 <sup>d</sup>

Three days after transfection, cells were fixed, stained with propidium iodide, and their DNA contents measured by flow cytometry. Cell cycle phase distributions were calculated with ModFit LT 3.0. Analyses were performed in duplicate and the data shown are the means  $\pm$  SE. SEPW1 siRNA-treated cells were compared to the control cells with a two-way ANOVA and Tukey's multiple comparisons test. Means within a column not sharing a superscript are significantly different ( $p < 0.05$ ). Representative pseudo-color density plots of events and cellular DNA content are shown in Supplemental Figure S2.

1045, and Tyr-1068 is associated with downstream signaling events [21,45]. Control and SEPW1-depleted RWPE-1 cells were starved of EGF overnight, re-supplied with 100 ng/mL EGF, and then analyzed with Western blots for total EGFR, p-Tyr-992-EGFR, p-Tyr-1045-EGFR, and p-Tyr-1068-EGFR. SEPW1 silencing decreased EGF-induced phosphorylation of the receptor on all three Tyr residues investigated and decreased total EGFR (Fig. 1). Because lower phospho-EGFR could merely reflect the amount of total EGFR, we also examined the ratio of phospho-EGFR/total EGFR. At 5 min, when EGFR phosphorylation was maximal, SEPW1 depletion decreased the ratio of phospho-EGFR/total EGFR for p-Tyr-992-EGFR, p-Tyr-1045-EGFR, and p-Tyr-1068-EGFR by 43%, 79%, and 63%, respectively, indicating EGFR auto-phosphorylation was decreased to a greater degree than total EGFR. This probably reflects the fact that auto-phosphorylation requires two EGFR monomers to form a dimer, and, is thus a second-order process with respect to EGFR concentration. Therefore, a relatively small change in total EGFR causes a much larger change in the rate of auto-phosphorylation. To guard against off-target effects, we repeated these experiments with a second siRNA targeted to a different sequence in SEPW1 (s363). EGFR phosphorylation at all three sites was decreased by SEPW1 siRNA s363 (Supplemental Figure S4), confirming this effect is specific to SEPW1 depletion.

### 3.3. SEPW1 overexpression enhances EGFR auto-phosphorylation

To ensure the effects of SEPW1 siRNA on EGFR auto-phosphorylation were not due to RNAi artifacts, we checked whether transient overexpression of SEPW1 would have the opposite effect. Overexpressing wild-type SEPW1 containing the N-terminal selenocysteine residue increased SEPW1 protein by approximately three-fold in RWPE-1 cells (Fig. 2). Cells transfected with the SEPW1 overexpression vector or empty vector were starved of EGF overnight, and then stimulated with 100 ng/mL EGF. Five minutes after EGF addition, EGFR auto-phosphorylation on Tyr 1068 and Tyr 1045 was 2.7- and 1.8-fold greater, respectively, in SEPW1-overexpressing cells compared to empty vector-transfected control cells and remained higher throughout the time course. However, total EGFR levels were not significantly increased by SEPW1 overexpression. The fact that SEPW1 overexpression had an opposite effect on EGFR auto-phosphorylation from SEPW1 depletion indicates the effect of siRNA on EGFR auto-phosphorylation was specifically due to altered expression of SEPW1 and was not an artifact of RNAi technology.

### 3.4. SEPW1 depletion blocks EGF-stimulated activation of downstream protein kinases

EGF binding to EGFR activates several signaling pathways. To assess the effect of SEPW1 depletion on pathways downstream from the EGFR,

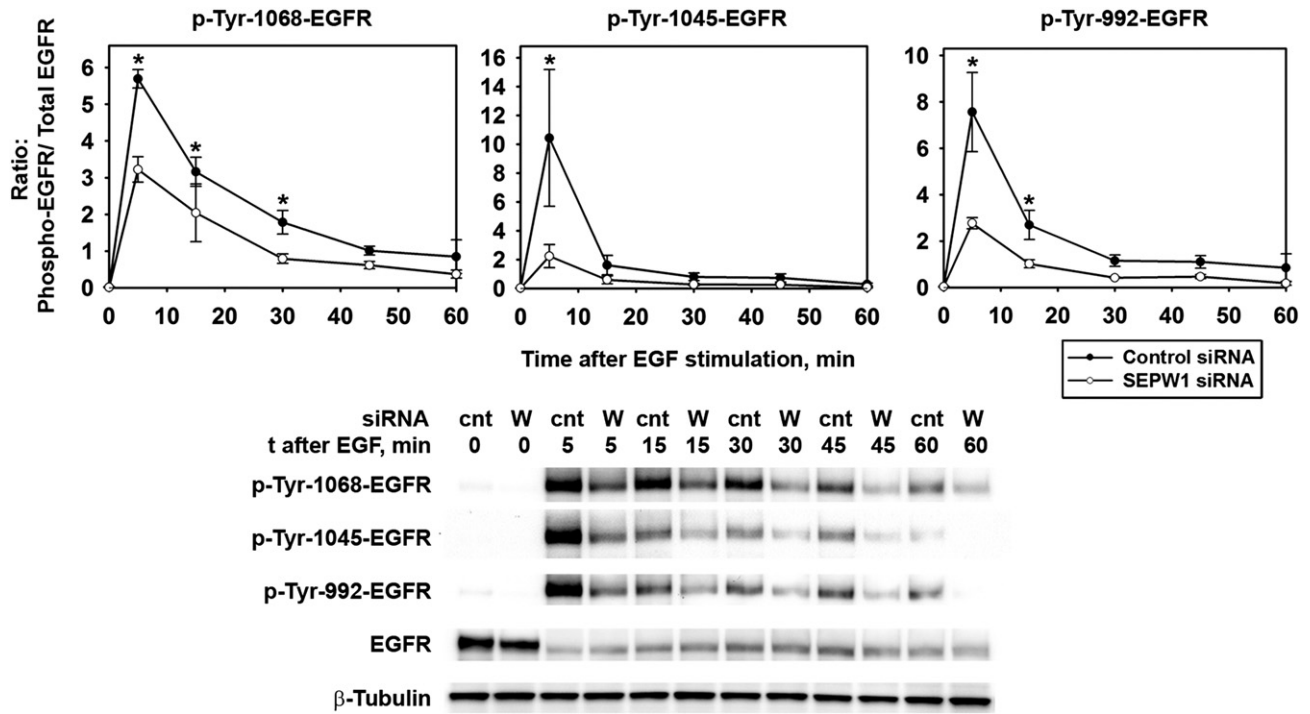


**Fig. 1.** SEPW1 depletion inhibits auto-phosphorylation of the EGF receptor. Two days after transfection with SEPW1 siRNA (open circles) or non-targeting control siRNA (solid circles), RWPE-1 cells were starved in EGF-free medium overnight, and then stimulated with medium containing 100 ng/mL EGF. Cells were lysed at 0, 5, 15, 30, 45 and 60 min post-EGF stimulation and the lysates were analyzed with Western blots using the indicated phospho-specific and pan-specific antibodies for EGFR.  $\beta$ -Tubulin served as a loading control. Because total EGFR also decreased with SEPW1 depletion, the data are displayed as ratios of phospho-EGFR/total EGFR. A representative immunoblot from a single experiment (lower panel; cnt, non-targeting control siRNA; W, SEPW1 siRNA) and the averages  $\pm$  SE from three independent experiments conducted with two SEPW1 siRNAs and two control siRNAs (upper panel) are shown. Asterisks indicate the time points at which EGFR phosphorylation was significantly different between the control siRNA and SEPW1 siRNA ( $p < 0.05$ , two-way ANOVA with Tukey's test). Results from individual SEPW1 and control siRNAs are shown in Supplemental Figures S3 and S4.

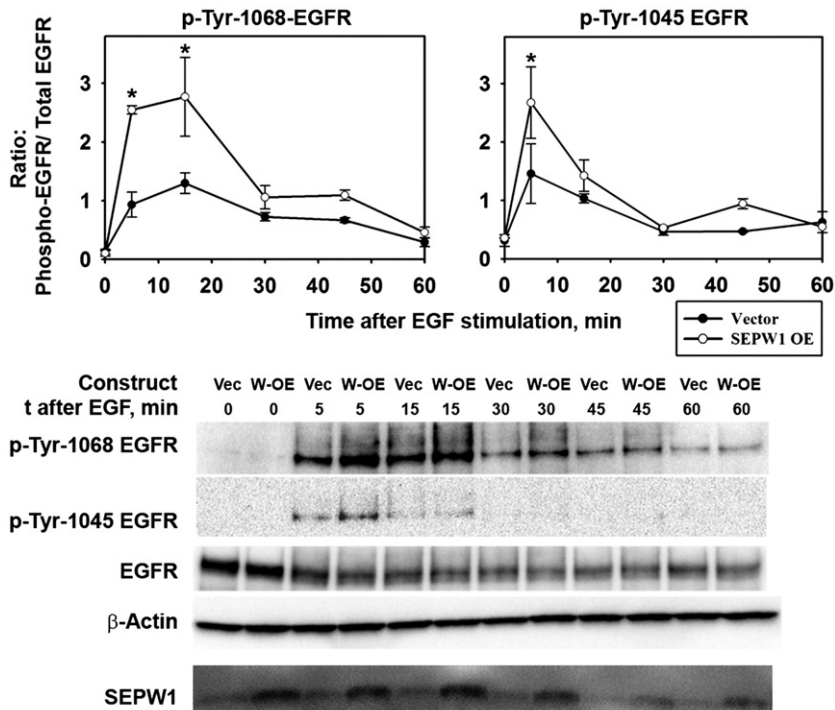


**Fig. 2.** SEPW1 overexpression enhances auto-phosphorylation of the EGF receptor. One day after transfection with a SEPW1 overexpression construct (open circles) or empty vector (solid circles), RWPE-1 cells were starved in EGF-free medium overnight, and then stimulated with medium containing 100 ng/mL EGF. Cells were lysed at 0, 5, 15, 30, 45 and 60 min post-EGF stimulation and the lysates were analyzed with Western blots using the indicated phospho-specific and pan-specific antibodies for EGFR.  $\beta$ -Actin served as a loading control. The data are displayed as ratios of phospho-EGFR/total EGFR. A representative immunoblot from a single experiment (lower panel; Vec, empty vector; W-OE, SEPW1 overexpression vector) and the averages  $\pm$  SE from three independent experiments (upper panel) are shown. Asterisks indicate the time points at which EGFR phosphorylation was significantly different between the vector control and SEPW1 overexpression ( $p < 0.05$ , two-way ANOVA with Tukey's test).

**Table 3**  
SEPW1 depletion attenuates EGF-stimulated activation of downstream protein kinases.

Activated kinase	Control siRNAs	SEPW1 siRNAs
Pan Ser(P)-Akt	1400 ± 311	667 ± 67
Ser(P)-133-CREB	613 ± 83	274 ± 64
Thr(P)-202/Tyr(P)-204-ERK1	1364 ± 117	562 ± 290
Thr(P)-185/Tyr(P)-187-ERK2	3233 ± 255	978 ± 607
Ser(P)-21/Ser(P)-9-GSK3- $\alpha/\beta$	1006 ± 117	479 ± 109
Ser(P)-9-GSK-3 $\beta$	1509 ± 459	547 ± 369
Ser(P)-360-MSK2	643 ± 22	229 ± 40
Thr(P)-180/Tyr(P)-182-p38 $\alpha$	646 ± 31	253 ± 31
Ser(P)-380-RSK1	941 ± 2	415 ± 87

Two days after transfection with two non-targeting siRNAs (Control #1 and Control #2), or two different siRNAs for SEPW1 (s361 and s363), cells were starved of EGF overnight, and then stimulated with 100 ng/mL EGF for 1 h. The cells were lysed, and lysates were hybridized to Proteome Profiler Human Phospho-MAPK antibody arrays. Phosphorylation of nine kinases listed in the table above was significantly decreased due to SEPW1 depletion with either siRNA ( $p < 0.05$ , two-way ANOVA and Tukey's multiple comparisons test). The data shown are array spot densitometry averages from the two controls or SEPW1 siRNAs  $\pm$  SE. Densitometry values for all the protein kinases from each individual siRNA are listed in *Supplemental Table S1*, and the image of the arrays is displayed in *Supplemental Figure S5*.

we used phosphospecific antibody arrays to simultaneously measure the activating phosphorylations on 26 protein kinases in starved cells stimulated with EGF for 60 min. EGF treatment of cells transfected with two different non-targeting control siRNAs induced phosphorylation of most of the kinases on the array (*Supplemental Figure S5*). Transfection of cells with either of two siRNAs targeting different sequences in the SEPW1 mRNA significantly suppressed EGF-stimulated phosphorylation of nine out of 26 kinases on the array (**Table 3**), confirming that SEPW1 depletion inhibits transmission of the EGF signal to multiple downstream pathways.

### 3.5. SEPW1 depletion decreases EGF-induced EGFR dimers

EGFR tyrosine kinase is fully active only when dimerized, either with another molecule of EGFR or with another receptor tyrosine kinase. EGF binding stabilizes and reconfigures EGFR dimers, thus activating the tyrosine kinase activity and initiating intracellular signaling [15]. When EGF-starved RWPE-1 cells were treated with the membrane-impermeable crosslinking reagent BS<sup>3</sup> without the addition of EGF, EGFR-immunoreactive high molecular weight signals could not be detected in control or SEPW1-silenced cells (left lanes in **Fig. 3**). EGF treatment induced a prominent EGFR-immunoreactive band at the dimer molecular weight of approximately 340 kDa in control cells that was greatly diminished (by  $84 \pm 14\%$ ) in SEPW1-depleted cells (**Fig. 3**).

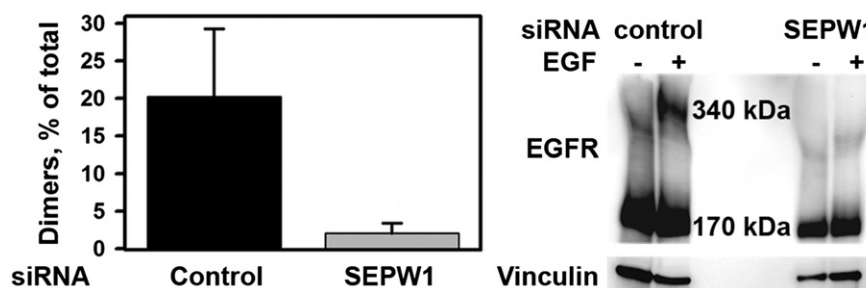


**Fig. 3.** SEPW1 depletion inhibits formation of EGFR dimers. Two days after transfection with SEPW1 siRNA or non-targeting control siRNA, RWPE-1 cells were starved in EGF-free medium overnight, incubated with cold medium containing 100 ng/mL EGF for 30 min at 4 °C, and treated with 3 mM BS<sup>3</sup> for 2 h at 4 °C as detailed under *Materials and methods*. Lysates were analyzed with Western blots using pan-specific antibodies for EGFR. Quantitative densitometry was conducted to estimate the chemiluminescence of EGFR monomers at 170 kDa and EGFR dimers at (approximately) 340 kDa. The percentage of dimers formed with each siRNA treatment was calculated from the total of monomer and dimer intensities. The experiment was conducted twice. A representative immunoblot from a single experiment is shown.

### 3.6. SEPW1 depletion inhibits EGF-induced EGFR endocytosis

EGFR is rapidly internalized by endocytosis after EGF binding [16]. We treated EGF-starved RWPE-1 cells with fluorescently-labeled EGF and examined them by confocal microscopy. Five minutes after addition of labeled EGF, SEPW1-depleted cells contained only about 40% as much fluorescent EGF per cell (**Fig. 4A**), indicating that EGFR endocytosis was suppressed in SEPW1-depleted cells.

### 3.7. SEPW1 depletion decreases surface expression of EGFR

Although EGFR at the plasma membrane can be imaged with a confocal microscope, the resolution is not adequate to differentiate EGFR actually on the extracellular surface from receptor in vesicles closely associated with the membrane. We used a monoclonal antibody specific for an epitope on the receptor's extracellular domain to label surface EGFR in continuously growing RWPE-1 cells and then measured the amount of surface EGFR per cell by flow cytometry. We tracked EGFR membrane expression prior to siRNA transfection, and on three consecutive days after transfection (**Fig. 4B**). Two days after transfection, the average amount of surface EGFR on SEPW1-depleted cells dropped to 54% of the level on control cells, and extracellular EGFR remained significantly low in SEPW1-silenced cells on the third day.

### 3.8. SEPW1 depletion accelerates EGFR degradation

Internalized EGFR is trafficked through endosomes, some portion is recycled, and then eventually the receptor is sorted to lysosomes for degradation. When protein synthesis is inhibited, the rate of disappearance of EGFR from cells is an indication of the receptor's rate of degradation. We treated continuously growing RWPE-1 cells with cycloheximide to inhibit synthesis of new protein and measured total EGFR protein for 6 h (**Fig. 5**). In control cells, EGFR decreased with an apparent first-order half-life of  $9.4 \pm 1.5$  h, whereas the apparent half-life was decreased to  $3.3 \pm 0.2$  h in SEPW1-depleted cells ( $p = 0.02$ ;  $n = 3$ , two-tailed, two sample equal variance *t*-test). Thus, the rate of EGFR degradation was increased approximately three-fold in SEPW1-depleted cells.

### 3.9. SEPW1 depletion increases EGFR ubiquitination

EGFR endocytosis stimulated by high-dose EGF is tightly coupled to ubiquitination of the receptor [17]. After internalization, subsequent trafficking of EGFR is determined largely by its ubiquitination state [10], which is dynamically regulated through the action of ubiquitin ligase and de-ubiquitinase enzymes [18]. Western blots of immunoprecipitated EGFR showed the receptor lacked detectable

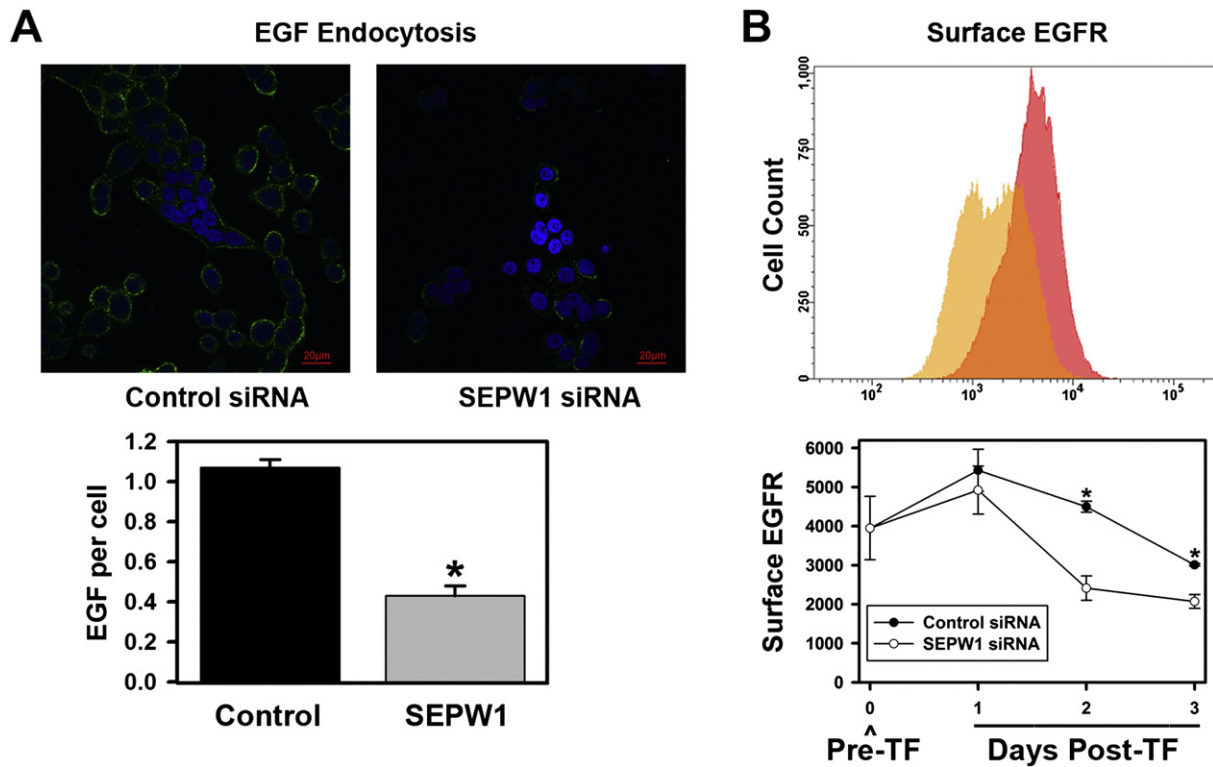


**Fig. 4.** EGFR endocytosis and surface EGFR expression are decreased by SEPW1 depletion. A—Two days after transfection with SEPW1 siRNA or a non-targeting control siRNA, RWPE-1 cells grown on coverslips were starved in EGF-free medium overnight, and stimulated with basal medium containing 970 ng/mL Alexa Fluor 488-labeled EGF for 5 min. The coverslips were processed, imaged, and EGF signal per cell was calculated as described under [Materials and methods](#). At least 100 cells per siRNA treatment were analyzed in each experiment from duplicate slides, and the experiment was conducted three times. The asterisk indicates SEPW1-silenced cells had significantly less endocytosed EGF compared to controls 5 min after fluorescent EGF addition ( $p < 0.001$ , two-way ANOVA with Tukey's test). Alexa Fluor 488-EGF is displayed as green and nuclei as blue. B—RWPE-1 cells grown continuously in medium supplemented with 5 ng/mL EGF were harvested and fixed before siRNA transfection (Pre-TF), and on Days 1, 2, and 3 post-transfection (Days Post-TF). The cells were then stained, and analyzed for cell surface EGFR by flow cytometry. The experiment was conducted twice, and the samples were run in duplicate. Representative histograms of SEPW1-silenced cells (yellow) and control cells (red) two days after transfection are shown. The asterisks indicate SEPW1-depleted cells had significantly lower surface EGFR expression on Days 2, and 3 post-transfection ( $p < 0.02$ , two-way ANOVA with Tukey's test).

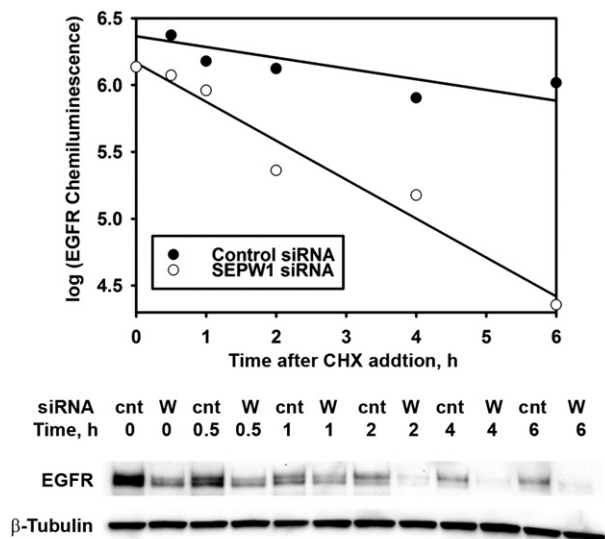


**Fig. 5.** SEPW1 depletion increases EGFR turnover rate. Three days after transfection with SEPW1 siRNA (open circles) or non-targeting control siRNA (solid circles), RWPE-1 cells were incubated with medium containing 60 mg/mL cycloheximide (CHX) to inhibit protein synthesis. Lysates were collected before (0 h) and at 0.5 h, 1 h, 2 h, 4 h and 6 h after CHX addition, and analyzed with Western blots using pan-specific EGFR antibodies.  $\beta$ -Tubulin served as a loading control. The experiment was repeated three times. A representative immunoblot from a single experiment and the regression of log EGFR chemiluminescence versus time from the corresponding blot is shown (cnt, non-targeting control siRNA; W, SEPW1 siRNA).

ubiquitin in starved cells, and was modified with ubiquitin shortly after EGF stimulation (Fig. 6). Two minutes after adding EGF, the EGFR in SEPW1-depleted cells was modified with three times as much ubiquitin as in control cells, indicating that SEPW1 depletion increases ubiquitination of EGFR. In order to guard against off-target RNAi effects, we confirmed these results with a second siRNA targeted to a different sequence in SEPW1 mRNA (s363). EGFR ubiquitination was increased by SEPW1 siRNA s363 similarly to siRNA s361 (Supplementary Figure S6). These results suggest SEPW1 either inhibits the process of ubiquitination or enhances removal of ubiquitin from the receptor.

### 3.10. SEPW1 depletion alters expression of genes in the EGFR pathway

We used whole genome DNA microarrays to assess the effect of SEPW1 depletion on gene expression in RWPE-1 cells. EGFR itself and IGF1R, which cross-activates EGFR, were up-regulated (Table 4). Also up-regulated were two EGFR ligands – TGF $\alpha$  and EGF – containing fibulin-like extracellular matrix protein 1, along with vascular endothelial growth factor A and transforming growth factor beta 1, whose receptors both transactivate the EGFR [19,20]. Two genes required for receptor endocytosis – RAB5A and EEA1 – were also up-regulated in SEPW1-depleted cells. Thus, the EGF receptor itself, an EGFR-transactivating receptor, two EGFR ligands, two EGFR-transactivating ligands, and two EGFR trafficking factors were up-regulated in SEPW1-depleted cells, suggesting a compensatory response to the blockade in EGF signaling caused by SEPW1 depletion.

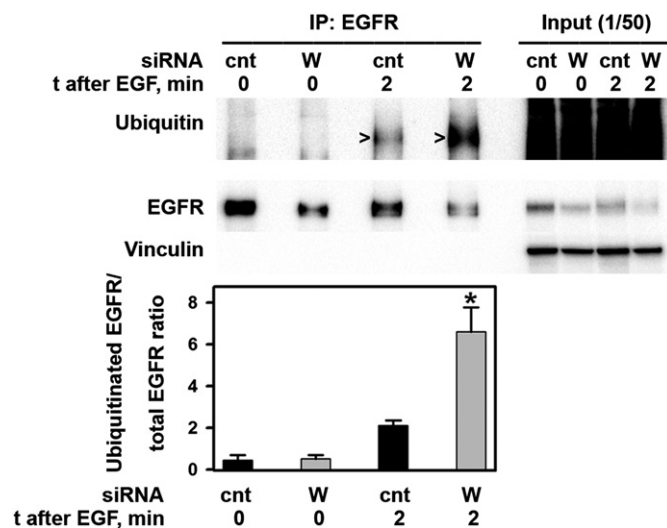


**Fig. 6.** EGFR ubiquitination is increased by SEPW1 depletion. Two days post-transfection with SEPW1 siRNA s361 or a non-targeting control siRNA, RWPE-1 cells were starved overnight, incubated with medium containing 0 or 100 ng/mL EGF for 2 min, and then immediately lysed. EGFR was immunoprecipitated from the lysates and the immunoprecipitates were analyzed for ubiquitin and EGFR by immunoblotting. The experiment was repeated four times. Arrowheads indicate the approximate position of ubiquitinated EGFR. SEPW1-silenced cells had significantly more ubiquitinated EGFR ( $p = 0.037$ ; two-way ANOVA with Tukey's test).

#### 4. Conclusions and discussion

We have presented evidence that SEPW1 is involved in EGFR signaling. Silencing SEPW1 inhibited EGF-stimulated cell cycle entry in breast and prostate epithelial cells. In addition, SEPW1 depletion inhibited dimerization, auto-phosphorylation and endocytosis of EGFR, decreased total and surface EGFR, and attenuated EGF-stimulated activation of downstream protein kinases, but increased ubiquitination and degradation of EGFR. Importantly, overexpressing SEPW1 had an opposite effect and increased EGFR phosphorylation. These results suggest SEPW1 regulates EGFR ubiquitination, which controls endosomal trafficking and recycling of the receptor, thus determining surface EGFR expression and the cell's responsiveness to EGF.

In the current model of EGFR activation, auto-phosphorylation of the receptor cytoplasmic domain causes binding of Cbl ubiquitin ligase and other proteins, receptor ubiquitination, and receptor internalization [21]. Once internalized the receptor may continue signaling, or be recycled to the cell surface, or be sorted to lysosomes for degradation. Consequently, trafficking of the receptor through endosomes controls a cell's sensitivity to EGF and enables the spatial and temporal

**Table 4**  
SEPW1 depletion alters expression of genes in the EGFR pathway.

Symbol	Gene name	mRNA (% of control)
SEPW1	Selenoprotein W, 1	43%
EFEMP1	EGF-containing fibulin-like extracellular matrix protein 1	270%
IGF1R	Insulin-like growth factor 1 receptor	191%
TGFB1	Transforming growth factor, beta 1	178%
TGFA	Transforming growth factor, alpha	164%
EGFR	Epidermal growth factor receptor	145%
VEGFA	Vascular endothelial growth factor A	145%
RAB5A	Member RAS oncogene family	164%
EEA1	Early endosome antigen 1	155%

RWPE-1 cells were transfected separately with three siRNAs targeting different sequences in SEPW1 mRNA, or a non-targeting control siRNA. RNA was extracted and labeled for analysis on Affymetrix GeneChips as described under [Materials and methods](#). Genes shown were called significantly changed by GCOS ( $p < 0.002$ ) for all three SEPW1 siRNAs compared to the control siRNA. Microarray data from individual siRNAs are shown in [Supplemental Table S2](#).

regulation of EGFR signaling [22]. After internalization, ubiquitinated EGFR is sorted to late endosomes and thence to lysosomes for degradation, whereas de-ubiquitinated EGFR is sorted to recycling endosomes, stripped of ligand and then returned to the plasma membrane for reuse.

Our results indicate SEPW1 antagonizes EGFR ubiquitination, either by inhibiting ubiquitination, or by enhancing de-ubiquitination. The totality of the evidence suggests SEPW1 most likely enhances de-ubiquitination. Silencing SEPW1 decreased every aspect of EGFR activation we measured except EGFR ubiquitination and EGFR degradation, tightly linked processes that were both up-regulated in SEPW1-depleted cells. EGFR endocytosis initiated by high dose EGF is preceded by, and is dependent on, ubiquitination of the receptor [23]. The fact that SEPW1 silencing decreased EGFR endocytosis and increased EGFR ubiquitination at the same time suggests that SEPW1 enhances de-ubiquitination of endosomal EGFR after endocytosis, rather than inhibiting EGFR ubiquitination before or during endocytosis.

The native biochemical activity and molecular function of SEPW1 remain obscure. The best characterized molecular interactions of SEPW1 are with 14-3-3 proteins, a family of phosphoprotein-binding proteins with diverse regulatory functions in the cell. 14-3-3 proteins have multiple functions in EGFR signaling: 14-3-3 $\zeta$  interacts directly with EGFR in fibroblasts [24] and inhibits Raf – the MAP3K target of EGFR-activated Ras [25]; dominant-negative 14-3-3 $\zeta$  blocks EGFR-mediated ERK activation by serum [26]; and, 14-3-3 $\gamma$  regulates both the MAPK and the PI3K/Akt pathways [27] downstream of EGFR. SEPW1 binds to 14-3-3 proteins [28] and is hypothesized to control their function by reacting with, or regulating the oxidation state of, an exposed Cys residue [29]. Alterations of 14-3-3 redox state and/or conformation by SEPW1 have been invoked to explain how SEPW1 knockdown enhances binding of 14-3-3 to CDC25B [30] and mTORC [31], which inhibits the activities of both targets. It is tempting to speculate that 14-3-3 may have a similar role in this pathway.

Ubiquitin-specific protease 8 (USP8) is one of two deubiquitinases that remove ubiquitin from endosomal EGFR [32]. EGFR activation causes USP8 to become phosphorylated and to associate with EGFR on endosomes where it dynamically regulates EGFR ubiquitination state during trafficking. Depletion of USP8 with siRNA inhibits EGFR activation and increases EGFR degradation [32], similar to the effect of depleting SEPW1, and suggests the possibility SEPW1 might regulate USP8. 14-3-3 binds to USP8 in a phosphorylation-dependent manner and inhibits its catalytic activity [33]. If SEPW1 acts as proposed for CDC25B and mTORC, then SEPW1 could cause 14-3-3 to dissociate from USP8, relieving the inhibition and increasing de-ubiquitination of EGFR. Such a mechanism would be consistent with the observed increase in EGFR ubiquitination when SEPW1 is silenced.

When EGF and many other growth factors bind to their receptors,  $H_2O_2$  is produced due to the actions of NADPH oxidase and superoxide dismutase [34,35]. SEPW1 has glutathione-dependent  $H_2O_2$ -catabolizing antioxidant activity in vitro [36], but its in vivo role as an antioxidant has been questioned [37]. Indeed, chemical antioxidants and the antioxidant selenoproteins GPX1 and GPX4 have opposite effects on EGF signaling from SEPW1. Small molecule antioxidants inhibit EGFR auto-phosphorylation [34] and dimerization [38], while overexpression of the antioxidant selenoproteins GPX1 or GPX4 blocks EGF-stimulated S-phase entry [39,40] rather than enhancing EGFR activation like over-expression of SEPW1. To the extent that SEPW1 regulates oxidation-reduction, it appears to act more as a pro-oxidant than as an antioxidant in this system.

EGF is an important promoter of cell cycle progression. Drugs that block EGF binding or inhibit EGFR tyrosine kinase activity cause G1 arrest and apoptosis in cancer cells. We observed a profound G1 arrest after withdrawal of EGF ([Tables 1 and 2](#)), but we did not observe significant numbers of cells with a sub-G0/G1 DNA content that would indicate apoptosis, perhaps because RWPE-1 cells are normal, non-cancerous prostate cells ([Figures S1 and S2, Supplemental Materials](#)).

SEPW1 silencing substantially blocked EGF-stimulated proliferation in breast and prostate epithelial cells, the cells that give rise to most tumors in these tissues. This is consistent with recent reports that SEPW1 is over-expressed in tumors [41] and that knockdown of SelW (the mouse homologue of SEPW1) increases sensitivity to anti-cancer drugs [30]. In a previous study, mice fed a selenium-deficient diet had greatly reduced expression of SelW and increased expression of the EGFR ligand Creld1 [42], suggesting dietary selenium regulates EGFR signaling in-vivo. The ubiquitous expression and evolutionary conservation of SEPW1 suggest it may have an ancient and essential function. Knowledge of the molecular function of SEPW1 and the mechanisms by which it modulates EGFR ubiquitination should improve our understanding of the complex relationship between selenium intake and cancer risk.

## Funding

This work was supported by the United States Department of Agriculture CRIS Project 5306-51530-018-00D.

## Competing interests

None of the authors have financial or other contractual agreements that might cause conflicts of interest or be perceived as causing conflicts of interest. Mention of trade names or commercial products in this publication is solely for the purpose of providing specific information and does not imply recommendation or endorsement by the U.S. Department of Agriculture. The opinions expressed herein represent those of the authors and do not necessarily represent those of the U.S. Department of Agriculture. The USDA is an equal opportunity provider and employer.

## Transparency document

The Transparency document associated with this article can be found, in the online version.

## Acknowledgements

We gratefully appreciate Leslie Hall's excellent technical assistance in supporting the conduct of our study. The UC Davis Comprehensive Cancer Center Gene Expression Resource supported by NCI Cancer Center Support Grant P30 CA93373 performed the microarray labeling, hybridizations and scanning.

## Appendix A. Supplementary data

Supplementary data to this article can be found online at <http://dx.doi.org/10.1016/j.bbamcr.2015.02.016>.

## References

- [1] S. Cohen, G. Carpenter, L. King Jr., Epidermal growth factor-receptor-protein kinase interactions. Co-purification of receptor and epidermal growth factor-enhanced phosphorylation activity, *J. Biol. Chem.* 255 (1980) 4834–4842.
- [2] R. Levi-Montalcini, S. Cohen, Effects of the extract of the mouse submaxillary salivary glands on the sympathetic system of mammals, *Ann. N. Y. Acad. Sci.* 85 (1960) 324–341.
- [3] A.B. Singh, R.C. Harris, Autocrine, paracrine and juxtacrine signaling by EGFR ligands, *Cell. Signal.* 17 (2005) 1183–1193.
- [4] J.V. Olsen, B. Blagoev, F. Gnad, B. Macek, C. Kumar, P. Mortensen, et al., Global, in vivo, and site-specific phosphorylation dynamics in signaling networks, *Cell* 127 (2006) 635–648.
- [5] J. van der Veecken, S. Oliveira, R.M. Schifferlers, G. Storm, P.M. van Bergen En Henegouwen, R.C. Roovers, Crosstalk between epidermal growth factor receptor and insulin-like growth factor-1 receptor signaling: implications for cancer therapy, *Curr. Cancer Drug Targets* 9 (2009) 748–760.
- [6] M.V. Karamouzis, P.A. Konstantinopoulos, A.G. Papavassiliou, Targeting MET as a strategy to overcome crosstalk-related resistance to EGFR inhibitors, *Lancet Oncol.* 10 (2009) 709–717.
- [7] C. Liebmann, EGF receptor activation by GPCRs: an universal pathway reveals different versions, *Mol. Cell. Endocrinol.* 331 (2011) 222–231.
- [8] E. Burova, K. Vassilenko, V. Dorosh, I. Gonchar, N. Nikolsky, Interferon gamma-dependent transactivation of epidermal growth factor receptor, *FEBS Lett.* 581 (2007) 1475–1480.
- [9] B. Mohapatra, G. Ahmad, S. Nadeau, N. Zutshi, W. An, S. Scheffe, et al., Protein tyrosine kinase regulation by ubiquitination: critical roles of Cbl-family ubiquitin ligases, *Biochim. Biophys. Acta* 2013 (1833) 122–139.
- [10] M.H. Wright, I. Berlin, P.D. Nash, Regulation of endocytic sorting by ESCRT-DUB-mediated deubiquitination, *Cell Biochem. Biophys.* 60 (2011) 39–46.
- [11] W.C. Hawkes, T.T.Y. Wang, Z. Alkan, B.D. Richter, K. Dawson, Selenoprotein W modulates control of cell cycle entry, *Biol. Trace Elem. Res.* 131 (2009) 229–244.
- [12] W.C. Hawkes, I. Printsev, Z. Alkan, Selenoprotein W depletion induces a p53- and p21-dependent delay in cell cycle progression in RWPE-1 prostate epithelial cells, *J. Cell. Biochem.* 113 (2012) 61–69.
- [13] W.C. Hawkes, Z. Alkan, Delayed cell cycle progression from SEPW1 depletion is p53- and p21-dependent in MCF-7 breast cancer cells, *Biochem. Biophys. Res. Commun.* 413 (2011) 36–40.
- [14] W.C. Hawkes, Z. Alkan, Delayed cell cycle progression in selenoprotein W depleted cells is regulated by a Mitogen-Activated Protein Kinase Kinase 4 (MKK4)-p38/c-Jun NH2-terminal kinase (JNK)-p53 pathway, *J. Biol. Chem.* 287 (2012) 27371–27379.
- [15] N.F. Endres, K. Engel, R. Das, E. Kovacs, J. Kuriyan, Regulation of the catalytic activity of the EGF receptor, *Curr. Opin. Struct. Biol.* 21 (2011) 777–784.
- [16] A. Sorkin, L.K. Goh, Endocytosis and intracellular trafficking of ErbBs, *Exp. Cell Res.* 315 (2009) 683–696.
- [17] L.K. Goh, A. Sorkin, Endocytosis of receptor tyrosine kinases, *Cold Spring Harb. Perspect. Biol.* 5 (2013) a017459.
- [18] J.H. Hurley, H. Stenmark, Molecular mechanisms of ubiquitin-dependent membrane traffic, *Annu. Rev. Biophys.* 40 (2011) 119–142.
- [19] K.D. Rodland, N. Bollinger, D. Ippolito, L.K. Opreko, R.J. Coffey, R. Zangar, et al., Multiple mechanisms are responsible for transactivation of the epidermal growth factor receptor in mammary epithelial cells, *J. Biol. Chem.* 283 (2008) 31477–31487.
- [20] E. Lee, J.Y. Yi, E. Chung, Y. Son, Transforming growth factor beta(1) transactivates EGFR via an H(2)O(2)-dependent mechanism in squamous carcinoma cell line, *Cancer Lett.* 290 (2010) 43–48.
- [21] I.H. Madshus, E. Stang, Internalization and intracellular sorting of the EGF receptor: a model for understanding the mechanisms of receptor trafficking, *J. Cell Sci.* 122 (2009) 3433–3439.
- [22] N. Taub, D. Teis, H.L. Ebner, M.W. Hess, L.A. Huber, Late endosomal traffic of the epidermal growth factor receptor ensures spatial and temporal fidelity of mitogen-activated protein kinase signaling, *Mol. Biol. Cell* 18 (2007) 4698–4710.
- [23] K. Haglund, I. Dikic, The role of ubiquitylation in receptor endocytosis and endosomal sorting, *J. Cell Sci.* 125 (2012) 265–275.
- [24] M.P. Oksvold, H.S. Huitfeldt, W.Y. Langdon, Identification of 14-3-3zeta as an EGF receptor interacting protein, *FEBS Lett.* 569 (2004) 207–210.
- [25] N. Dumaz, R. Marais, Protein kinase A blocks Raf-1 activity by stimulating 14-3-3 binding and blocking Raf-1 interaction with Ras, *J. Biol. Chem.* 278 (2003) 29819–29823.
- [26] H. Xing, S. Zhang, C. Weinheimer, A. Kovacs, A.J. Muslin, 14-3-3 proteins block apoptosis and differentially regulate MAPK cascades, *EMBO J.* 19 (2000) 349–358.
- [27] V.M. Radhakrishnan, J.D. Martinez, 14-3-3gamma induces oncogenic transformation by stimulating MAP kinase and PI3K signaling, *PLoS ONE* 5 (2010) e11433.
- [28] F.L. Aachmann, D.E. Fomenko, A. Soragni, V.N. Gladyshev, A. Dikiy, Solution structure of selenoprotein W and NMR analysis of its interaction with 14-3-3 proteins, *J. Biol. Chem.* 282 (2007) 37036–37044.
- [29] A. Dikiy, S.V. Novoselov, D.E. Fomenko, A. Sengupta, B.A. Carlson, R.L. Cerny, et al., SelT, SelW, SelH, and Rdx12: genomics and molecular insights into the functions of selenoproteins of a novel thioredoxin-like family, *Biochemistry* 46 (2007) 6871–6882.
- [30] Y.H. Park, Y.H. Jeon, I.Y. Kim, Selenoprotein W promotes cell cycle recovery from G2 arrest through the activation of CDC25B, *Biochim. Biophys. Acta* 2012 (1823) 2217–2226.
- [31] Y.H. Jeon, Y.H. Park, J.H. Kwon, J.H. Lee, I.Y. Kim, Inhibition of 14-3-3 binding to Rictor of mTORC2 for Akt phosphorylation at Ser473 is regulated by selenoprotein W, *Biochim. Biophys. Acta* 13 (2013) 00185–00187.
- [32] E. Mizuno, T. Iura, A. Mukai, T. Yoshimori, N. Kitamura, M. Komada, Regulation of epidermal growth factor receptor down-regulation by UBPY-mediated deubiquitination at endosomes, *Mol. Biol. Cell* 16 (2005) 5163–5174.
- [33] E. Mizuno, N. Kitamura, M. Komada, 14-3-3-dependent inhibition of the deubiquitinating activity of UBPY and its cancellation in the M phase, *Exp. Cell Res.* 313 (2007) 3624–3634.
- [34] Y.S. Bae, S.W. Kang, M.S. Seo, I.C. Baines, E. Tekle, P.B. Chock, et al., Epidermal growth factor (EGF)-induced generation of hydrogen peroxide. Role in EGF receptor-mediated tyrosine phosphorylation, *J. Biol. Chem.* 272 (1997) 217–221.
- [35] M. Giorgio, M. Trinei, E. Migliaccio, P.G. Pellicci, Hydrogen peroxide: a metabolic by-product or a common mediator of ageing signals? *Nat. Rev. Mol. Cell Biol.* 8 (2007) 722–728.
- [36] D. Jeong, T.S. Kim, Y.W. Chung, B.J. Lee, I.Y. Kim, Selenoprotein W is a glutathione-dependent antioxidant in vivo, *FEBS Lett.* 517 (2002) 225–228.
- [37] W. Xiao-Long, Y. Chuan-Ping, X. Kai, Q. Ou-Jv, Selenoprotein W depletion in vitro might indicate that its main function is not as an antioxidative enzyme, *Biochemistry (Mosc)* 75 (2010) 201–207.
- [38] H. Kamata, Y. Shibukawa, S.I. Oka, H. Hirata, Epidermal growth factor receptor is modulated by redox through multiple mechanisms. Effects of reductants and H<sub>2</sub>O<sub>2</sub>, *Eur. J. Biochem.* 267 (2000) 1933–1944.
- [39] D.E. Handy, E. Lubos, Y. Yang, J.D. Galbraith, N. Kelly, Y.Y. Zhang, et al., Glutathione peroxidase-1 regulates mitochondrial function to modulate redox-dependent cellular responses, *J. Biol. Chem.* 284 (2009) 11913–11921.



- [40] H.P. Wang, F.Q. Schafer, P.C. Goswami, L.W. Oberley, G.R. Buettner, Phospholipid hydroperoxide glutathione peroxidase induces a delay in G1 of the cell cycle, *Free Radic. Res.* 37 (2003) 621–630.
- [41] Y. Hu, H. Sun, J. Drake, F. Kittrell, M.C. Abba, L. Deng, et al., From mice to humans: identification of commonly deregulated genes in mammary cancer via comparative SAGE studies, *Cancer Res.* 64 (2004) 7748–7755.
- [42] D.H. Mallonee, C.A. Crowdus, J.L. Barger, K.A. Dawson, R.F. Power, Use of stringent selection parameters for the identification of possible selenium-responsive marker genes in mouse liver and gastrocnemius, *Biol. Trace Elem. Res.* 143 (2011) 992–1006.
- [43] V. Girish, A. Vijayalakshmi, Affordable image analysis using NIH Image/ImageJ, *Indian J. Cancer* 41 (2004) 47.
- [44] O. Gavet, J. Pines, Progressive activation of CyclinB1–Cdk1 coordinates entry to mitosis, *Dev. Cell* 18 (2010) 533–543.
- [45] Y.M. Agazie, M.J. Hayman, Molecular mechanism for a role of SHP2 in epidermal growth factor receptor signaling, *Mol. Cell. Biol.* 23 (2003) 7875–7886.